SUPPLEMENTARY INFORMATION

Dynamic Control of Strand Excision during Mismatch Repair

Yongmoon Jeon, Daehyung Kim, Juana Martín-López, Ryanggeun Lee, Jungsic Oh, Jeungphill Hanne, Richard Fishel, Jong-Bong Lee

SUPPLEMENTARY METHODS

Preparation of Proteins

HsMSH2-HsMSH6 - HsMSH2 WT (pFastBac™ 1; Invitrogen) and N-terminal His-tagged HsMSH6 WT (pFastBac™ HT A) were coexpressed in SF9 cells and purified by FPLC as previously described (1) with some modifications (2). Protein extracts were loaded into a Nickel column (Ni-NTA agarose, Qiagen) followed by PBE-94 column (PolyBuffer exchanger 94, Sigma) and eluted in two steps. Further contaminants were separated by Gel Filtration column (HiLoad™ 16/60 Superdex 200, GE Healthcare) and polished using MonoQ column (GE Healthcare). Peak fractions were dialyzed overnight against 25mM Hepes pH 7.8, 150mM NaCl, 1mM DTT, 0.1mM EDTA and 20% Glycerol. Protein concentration was determined based on the molar extinction coefficient (202,840 cm^{-1} M^{-1}) for HsMSH2-HsMSH6 and aliquots were frozen in liquid nitrogen and store at -80°C.

mEos3.2-HsMSH2-HsMSH6 - The mEos3.2 photoswitchable fluorescent protein and the HsMSH2 gene were inserted into a pBAD and pFastBac1 vectors, respectively. The fragments of mEos3.2 and HsMSH2 genes were amplified by PCR and ligated together. The mEos3.2-HsMSH2 fragment was cleaved by the restriction enzymes of BstAPI and SalI (NEB), which resulted in the fragment consisting of a full-mEos3.2 and a partial-HsMSH2 gene. The resulting fragment was inserted into an HsMSH2-pFastBac1 vector. The cloned mEos3.2-HsMSH2 was expressed and mEos3.2-HsMSH2-HsMSH6 proteins were purified as described for HsMSH2-HsMSH6.

HsMLH1-HsPMS2 - HsMLH1 (pFastBac™ 1; invitrogen) and HsPMS2 (pFastBac™ 1) were coexpressed in SF9 cells an. No additional tags were added to these proteins. HsMLH1-HsPMS2 naturally binds Ni-NTA agarose column and was eluted, passed through a PBE-94 column and loaded directly into a ssDNA-cellulose column (Affymetrix). HsMLH1-HsPMS2 was eluted in a single step and separated from remaining contaminant by Gel Filtration (Superdex

200). Fractions were polished by chromatography on MonoQ column and dialyzed in the same buffer described for HsMSH2-HsMSH6. Quantification was performed using the calculated molar extinction coefficient of the heterodimer: 90,650 cm^{-1} M^{-1} and aliquots were store at -80°C.

HsEXOI - A His_6-tag was added to the C-terminus of the HsEXOIb protein (pFastBac™ 1). Protein was expressed in SF9 cells and purified by avoiding direct dilution of the protein where possible. HsEXOIb was first loaded into a Heparin column (Heparin Sepharose 6 Fast Flow, GE Healthcare) in 20mM Potassium Phosphate buffer pH 7.5, 300mM NaCl, 10% Glycerol and proteinase inhibitors and eluted with a NaCl gradient. Peak fractions were loaded directly onto a Ni-NTA column, eluted in an Imidazole gradient containing 150mM NaCl followed by MonoS column (GE Healthcare). Fractions were overnight dialyzed in 20mM potassium Phosphate Buffer pH 7.5, 200mM NaCl, 1mM DTT, 0.1mM EDTA and 20% Glycerol. Protein concentration was calculated using the molar extinction coefficient for the protein: 55,810 cm^{-1} M^{-1}, and aliquots were frozen and store at -80°C.

HsRPA - HsRPA protein was purified as previously described (4) with several modifications (5). The pET11d-tRPA plasmid containing all HsRPA subunits was expressed in *E. coli* cells with 0.2% L-arabinose and 1mM IPTG. After 5 hours, cells were collected and resuspended in 30mM Hepes pH 7.5, 100mM KCl, 1mM DTT, 0.25mM EDTA, 0.01% NP-40, 1% Glycerol and proteinase inhibitors. Cells were lysed by sonication and cleared supernatant was loaded on an Affi-gel™ Blue Gel column (BioRad). After several washes with increased concentrations of KCl, followed by a wash containing 0.5M NaSCN, proteins were eluted in 30mM Hepes pH 7.5, 1.5M NaSCN, 1mM DTT, 0.25mM EDTA, 1% Glycerol, 0.01% NP-40 and protein inhibitors. Peak fractions were loaded directly on a Hydroxyapatite column (HAP; Macro-Prep Ceramic Hydroxyapatite, BioRad) and eluted with a potassium phosphate linear gradient containing 100mM KCl. Peak fractions fromm HAP were diluted to 150mM, loaded onto a MonoQ column (GE Health Care) and eluted with a linear KCl gradient. Proteins fractions were dialyzed in storage buffer: 20mM Hepes pH 7.5, 100mM NaCl, 0.5mM DTT and 10% Glycerol. Concentration was determined by Bradford method and aliquots were frozen in liquid nitrogen and store at -80°C.

DNA substrates

15.3 kb G-T mismatched DNA - Both ends of the DNA were modified with 5'-biotin and 5'-digoxigenin, respectively (6). The G/T mismatch is about 5.2 kb apart from the biotinylated nucleotide. For excision reactions with HsEXO1, a single nick was introduced by Nb.BbvC1

endonuclease (New England Biolabs), which is about 8 kb away from the mismatch site in 5'-digoxigenin direction. We first prepared two large fragments obtained from λ-phage DNA (New England Biolabs) cleaved by BsrG1 enzyme (New England Biolabs) and by Apa1 (Roche): one is 5.2 kb long and the other is 10.1 kb long. All oligos used for the DNA substrate are listed in Table S1. The 5.2-kb fragment was annealed and ligated with 5'-biotin, biotin linker and mismatch linker 1 using T4 DNA ligase (Roche). The 10.1-kb fragment was annealed and ligated with 5'-digoxigenin, digoxigenin linker and mismatch linker 2. These two parts were purified using Gel electrophoresis to remove free oligos and unwanted λ-phage DNA fragments (Gel: 0.5% agarose gel, Extraction: QIAquick Gel Extraction Kit, QIAGEN), separately. After the extraction these two parts were desalted using ethanol precipitation for increasing an efficiency of ligation. These two fragments of biotin-modified 5.2 kb and digoxigenin-modifed 10.1 kb were ligated with the oligos of mismatch linker 1 and mismatch linker 2 at a molar ratio of 1:1.2.

15.3 kb duplex DNA – To produce the fully duplex DNA the Mismatch linker 2 was replaced with the Duplex linker 1 in the 15.3 kb G/T mismatched DNA (Table S1).

21.5 kb, 22 kb and 23 kb G/T mismatched DNA - We constructed three G-T mismatched DNAs having various distances between the mismatch and a gap (about 0.5 kb, 1 kb and 2 kb). Short DNA fragments (0.5 kb, 1 kb, 2 kb) obtained by PCR were ligated with a long λ-based DNA fragment (21 kb), which results in G/T mismatched DNAs of 21.5 kb, 22 kb and 23 kb in length, respectively. The PCR fragments were amplified from the pcDNA 3.1 FLAG vector using AmpliTaq Gold 360 Master Mix (Applied Biosystems). PCR primers were designed to have a restriction site for Nt.BstNB1 (NEB) to make 5'-overhang on both sides of the PCR products, which was used for the efficient ligation with the 21-kb DNA fragment. The Amplified DNA fragments were purified by QIAquick PCR purification Kit (QIAGEN) according to manufacturer's instructions. After the purification, the DNA fragments were cleaved by Nt.BstNB1 and heated to 85°C, which resulted in 12-nt overhang away from the 3'-end of the upper strand and 12 nt away from the 3'-end of the lower strand. Following ethanol precipitation the DNA fragments were annealed and ligated with 3'-biotin PCR and mismatch linker 2 at a molar ratio of 1:50:50. The ligated DNA fragments were purified using Gel Electrophoresis (1% agarose, extracted using QIAquick Gel Extraction Kit, QIAGEN). The 21-kb long DNA fragments were obtained from λ-phage DNA by the cleavage of EcoR1 (New England Biolabs), which were desalted using ethanol precipitation and ligated with mismatch linker 1, 5'-dioxigenin EcoR1 and 5'-dioxigenin EcoR1 linker at a molar ratio of 1:150:500:250. The ligated 21 kb fragments were

purified and ligated with the prepared PCR products at a molar ratio of 1:1.2. The purified DNA substrates were stored at -20°C.

Single molecule flow stretching

All HsEXOI reactions were performed in Buffer A (40 mM Tris-HCl, pH 7.6, 5 mM $MgCl_2$, 120 mM KCl, 0.1 mg/ml BSA, 0.1 mM ADP, 1 mM ATP, 0.5 mM DTT). 1 mM ADP was substituted for ATP in experiments without ATP. A custom flow chamber was constructed for the flow-stretching experiments as described previously (7). A cover glass was functionalized with PEG-biotin and PEG (with a mass ratio of 1:100, Laysan Bio) to minimize the nonspecific binding of DNA substrates or proteins. The flow chamber with 25.0 X 3.0 X 0.1 mm dimension was built up with a slide glass washed by Acetone and the functionalized cover glass. To immobilize Biotin-labeled DNA substrates, NeutrAvidin in PBS (0.05 mg/ml, Thermo Scientific) was incubated in the flow chamber for 5 min and then the free NeutrAvidin molecules was washed out with a blocking buffer (20 mM Tris-HCl, pH 7.5, 2 mM EDTA, 50 mM NaCl, 0.0025% Tween 20 (v/v), 0.1 mg/ml BSA). DNA substrates were attached to the cover glass surface of the flow chamber via a biotin-streptavidin linkage by flowing a DNA (~0.5 pM) in the blocking buffer for 10 min using a syringe pump (0.04 ml/min, Harvard apparatus). Free DNA molecules in solution were removed by stringently washing (~0.2 ml of blocking buffer). Anti-digoxigenin (anti-digoxigenin Fab, Roche) coated super-paramagnetic beads (2.8 um in diameter, Invitrogen) were introduced to the flow chamber where DNA substrates were immobilized, which was linked to the digoxigenin-end of the DNA. Prior to the addition of proteins, free beads were removed by extensive washing (>2 ml of blocking buffer). A hydrodynamic force by laminar flow of the buffer was applied to a tethered bead at ~2.2 pN (7). The magnetic force generated by a ring-shaped rare earth magnet was also applied to a bead at ~ 1 pN for avoiding a nonspecific interaction between the bead and the surface (7). The net force acting on the bead was 2.5 pN. The bead linked to DNA was imaged using an optical microscope under a 10 x objective (N.A. = 0.40, Olympus). The image was recorded with a high-resolution CCD (RETIGA 2000R, Qimaging) using MetaVue (Molecular Devices) imaging software with a 1 s time resolution. The position of bead was determined with a high accuracy (~ 20 nm) by DiaTrack 3.03 (8). The data were analyzed by OriginPro8 (OriginLab) and Matlab 2013b (Mathworks).

The distribution of binned excision length by multiple exonucleases was fitted to a Gamma distribution. The mean value was obtained from mean = $k^*\theta$ with variance of $k^*\theta^2$, where k and θ are fitting parameters of a Gamma distribution:

$$f(x;k,\theta) = \frac{x^{k-1}e^{-x/\theta}}{\theta^k \Gamma(k)}$$

The standard error of the mean (s.e.) was obtained from $\sqrt{k} * \theta/\sqrt{N}$, where N is the number of molecules we analyzed.

Single molecule TIRF Imaging

The DNA substrates were immobilized to the quartz surface and all reactions were performed in Buffer A as described in the single molecule flow stretching. HsEXOI activity following a 60 min incubation was determined by the production of HsRPA-bound ssDNA that was imaged with 5 μg/ml Alexa647-labeled anti-HsRPA antibody (abcam; 10 min incubation). For reactions that contained HsRPA, the Alexa647-labeled anti-HsRPA antibody was added immediately following the 60 min incubation. For reactions that were performed in the absence of HsRPA, HsRPA (10 nM) was added immediately following the 60 min incubation for 10 min, followed by the Alexa647-labeled anti-HsRPA antibody. To image the dsDNA, Sytox Orange (20 nM; Thermo Fisher Scientific) was added in the flow chamber following the Alexa647-labeled anti-HsRPA antibody incubation. Alexa647 and Sytox Orange emission signals were imaged using a prism-type total internal reflection fluorescence microscope as previously described (2, 4). The emission signals were separated by a DV2 (Photometrics) and colocalized using a filter set (a 650 long pass dichroic mirror and two emission filters 600/37 & 676/37; Semrock). The time resolution was 100 ms. Fluorescence Images were analyzed using ImageJ and matlab 2013b (Mathworks)

The Relative Frequency was determined from the frequency of molecules under an MMR excision reaction condition (x) that displayed an Alexa647-HsRPA staining intensity equal or greater than one standard deviation of the average intensity found in the HsEXOI plus HsRPA reaction (≥HsEXOI*; Fig. S3, Lane 5) normalized to the frequency of molecules in the HsEXOI alone reaction that displayed an Alexa647-HsRPA staining intensity equal or greater than one standard deviation of the average intensity found in the HsEXOI plus HsRPA reaction $[N(x)_{\geq HsEXOI^*} \div N(x)_{T\bullet x}] \div [N_{HsEXOI \geq HsEXOI^*} \div N_{T\bullet HsEXOI}]$. Where: $N(x)_{\geq HsEXOI^*}$ = number of molecules observed under an MMR excision reaction condition (x) that displayed an Alexa647-HsRPA staining intensity equal or greater than one standard deviation of the average intensity found in the HsEXOI plus HsRPA reaction; $N(x)_{T\bullet x}$ = Total number of Sytox Orange stained molecules observed under an MMR excision reaction condition (x); $N_{HsEXOI \geq HsEXOI^*}$ = number of molecules in the HsEXOI alone reaction that displayed an Alexa647-HsRPA staining intensity equal or greater than one standard deviation of the average intensity found in the HsEXOI plus HsRPA

reaction; $N_{T•HsEXOI}$ = Total number of Sytox Orange stained molecules observed in the HsEXOI alone reaction, respectively.

Relative Frequency of Gap Extension - The FRET values in Fig. S4b and S4e were determined in Buffer A after a 30 min incubation that was followed by a stringently wash with 500 mM KCl for 10 min to remove bound proteins (e.g. HsRPA when present). The buffer was then exchanged for Buffer A with an oxygen scavenging system described in the PIFE experiment to determine fluorescent intensities.

The average FRET efficiency and its standard deviation (σ) were determined from the distribution of FRET efficiency in the absence of HsEXOI by a Gaussian fitting (Fig. S4b, top left: 0.25 ± 0.04; bottom left: 0.26 ± 0.04; Fig. S4e, top left: 0.29 ± 0.04; bottom left: 0.3 ± 0.03). The FRET states produced by HsEXOI with or without HsRPA were determined, with the FRET efficiency that was greater than a threshold value (= mean + 3σ; red dotted line) in the absence of HsEXOI. For example, in the absence of HsRPA there were 462 nick-DNA molecules with the FRET efficiency that was greater than 0.37 (0.25 + 3*0.04) out of 514 nick-DNA molecules (Fig. S4c). There existed FRET states with FRET efficiencies greater than the threshold value in the absence of HsEXOI: 15% at nick DNA and 1.5% at gapped DNA. To determine the Relative Frequency (Fig. S4c and S4f) we normailzed the Frequency of the FRET states with HsEXOI minus the background FRET states in the absence of HsEXOI using the relationship: $\langle Frequency \rangle = (\langle Frequency_{>threshold} \rangle - \langle Frequency_{BG} \rangle)/(100 - \langle Frequency_{BG} \rangle)$, where $\langle Frequency_{>threshold} \rangle$ is an average Frequency (%) for the FRET efficiency greater than the threshold in the presence of HsEXOI and $\langle Frequency_{BG} \rangle$ is an average Frequency (%) for the FRET efficiency greater than the threshold in the absence of HsEXOI. The normalized Frequencies are shown in Fig. S4c and S4f. To obtain the average Frequency, we analyzed five images for each condition.

Protein Induced Fluorescence Enhancement (PIFE)

DNA substrates for PIFE experiments **-** We prepared 40 bp long G/T mismatched DNA containing various ssDNA tails (0, 10, 30 and 40 dT) and 40 bp long duplex DNA without ssDNA tail. All the DNA substrates were modified with a Cy3 dye conjugated to a thymine base and a biotin to 5' end of the DNA. Four mismatched DNA substrates containing a single G/T mismatch in the middle of the duplex region. The DNA substrate without a mismatch has a blunt end. At the 5' end of G/T mismatched DNAs containing +0dT or +10dT tail and the duplex DNA, digoxigenin was modified to block the DNA end using Anti-Digoxigenin antibody (Roche).

All oligos were purchased from IDT (Integrated DNA Technologies, USA). DNA substrates were obtained by annealing paired top and bottom oligos listed in Table S2 at a molar ratio of 1:1.2 in the annealing buffer (10 mM Tris-HCl, pH 8.0, 100 mM NaCl, 1 mM EDTA) for a final concentration of 5 μM. An annealing process was conducted by heating at 95°C for 5 min and slowly cooling down to room temperature. The amino C6 dT-modified oligo was labeled with Cy3 (Monofunctional NHS-ester, GE Healthcare) as described previously (3).

The dwell time of HsMSH2-HsMSH6 on the DNA using PIFE - All reactions were performed in Buffer A (40 mM Tris-HCl, pH 7.6, 5 mM $MgCl_2$, 120 mM KCl, 0.1 mg/ml BSA, 0.1 mM ADP, 1 mM ATP, 0.5 mM DTT). A quartz slide was functionalized with PEG-biotin and PEG (1:40 w/w, Laysan Bio). The quartz surface of the flow chamber was coated with NeutrAvidin with the blocking buffer as described in the flow-stretching method. To immobilize the DNA substrates, 10 pM DNA in the blocking buffer was infused into the flow chamber for 5 min. After washing free DNA with the blocking buffer, we incubated 50 nM anti-digoxigenin antibody (Roche) or 20 nM RPA in the flow chamber for 10 min to block the end of the DNA. Before the reaction, free DNA, free anti-digoxigenin or free RPA in the solution was stringently washed out with the blocking buffer. To initiate HsMSH2-HsMSH6 binding to the DNA, HsMSH2-HsMSH6 in Buffer A was introduced into the flow chamber and incubated as described in the text. Emission signals of Cy3 excited with a 532 nm DPSS laser (Cobolt Samba, 100 mW) was imaged in a prism-type total internal reflection fluorescence microscope (Olympus IX-71, water-type 60x objective, NA = 1.2) and recorded using EMCCD (ImagEM C9100-13, Hamamatsu) and MetaMorph (Molecular Devices) imaging software in the presence of the oxygen scavenging system [0.8% (w/v) D-glucose (Sigma), 165 U/ml glucose oxidase (Sigma), 2,170 U/ml catalase (Sigma), 3mM Trolox] to minimize photobleaching and suppress photoblinking of Cy3 fluorophore. PIFE data were analyzed using IDL 6.4 (EXELIS VIS) and Matlab 2013b (MathWorks). The time resolution was adjusted ranging from 0.2 s to 2 s according to the lifetime of HsMSH2-HsMSH6 using a time-lapse method. For the time-lapse experiment, emission signals were collected for 100 ms (excitation on) and blocked for 0.9 s ~ 1.9 s (excitation off). This on and off cycles were lasted for 33 ~ 66 min. The shutter system (Uniblitz Shutter Systems), which was used to turn the excitation on and off, was synchronized with the EMCCD using its internal trigger and operated by MetaMorph.

Surface Plasmon Resonance (SPR) binding kinetic analysis.

A 82 bp mismatched DNA containing a 5'-biotin on one end was attached to a streptavidin coated SPR chip (Biacore, GE Healthcare) as previously described (2). HsMSH2-HsMSH6 or mEos3.2-HsMSH2-HsMSH6 protein was bound at indicated concentrations in Buffer A with 0.005% P20 (GE healthcare, BR100054), 0.2mg/ml Acetylated BSA (Promega, R3961).

Supplementary Table 1. Oligonucleotides used for flow-stretching.

	Name	Length	Strand sequence (5' to 3')	Modification
For Nicked 15kb G/T DNA	5'-digoxigenin	29 nt	GAA TGT ACG TGA GAA TCG AGA CCC AGG CC	5': Digoxigenin
	5'-digoxigenin linker	25 nt	TGG GTC TCG ATT CTC ACG TAC ATT C	-
	5'-biotin	17 nt	TTT GTC AAC GTC ATC TA	5': Biotin
	5'-biotin linker	19 nt	GTA CTA GAT GAC GTT GAC A	-
	Mismatch linker 1	47 nt	AGG TCG CCG CCC TTA CTT AGC AGA **T**CG AAC ACA **T**AG CAC ATA CTA GC	5': Phosphate **T**: GT mismatch
	Mismatch linker 2	47 nt	AGG TCG CCG CCC GCT AGT ATG TGC TAT GTG TTC G**G**T CTG CTA AGT AA	5': Phosphate **G**: GT mismatch
For Nicked 15kb Duplex DNA	5'-digoxigenin	29 nt	Same with above	Same with above
	5'-digoxigenin linker	25 nt	Same with above	Same with above
	5'-biotin	17 nt	Same with above	Same with above
	5'-biotin linker	19 nt	Same with above	Same with above
	Mismatch linker 1	47 nt	Same with above	Same with above
	Duplex linker 1	47 nt	AGG TCG CCG CCC GCT AGT ATG TGC TAT GTG TTC G**A**T CTG CTA AGT AA	5': Phosphate
For 21.5 kb, 22 kb, 23 kb G/T DNA	0.5 kb primer (F)	45 nt	GTC ATC TAC ATG GCT TGA CTC CCA TAG TCC CGC CCC TAA CTC CGC	5': Phosphate
	0.5 kb primer (R)	45 nt	GGG CGG CGA CCT GGA TGA CTC TTC CCC AAT GTC AAG CAC TTC CGG	5': Phosphate
	1 kb primer (F)	45 nt	GTC ATC TAC ATG GCT TGA CTC CTG GAA CAA CAC TCA ACC CTA TCT	5': Phosphate
	1 kb primer (R)	45 nt	GGG CGG CGA CCT GGA TGA CTC AGC AAT CGC GCA TAT GAA ATC ACG	5': Phosphate
	2 kb primer (F)	41 nt	GTC ATC TAC ATG GGA TGA CTC CCA AAC TGG AAC AAC ACT CA	5': Phosphate
	2 kb primer (R)	41 nt	GGG CGG CGA CCT GGA TGA CTC CGA GGA AGC GGA AGA GCG CC	5': Phosphate
	3'-biotin PCR	43 nt	CAT GTA GAT GAC GTT GAC AGC AGG GAG GAT TTC AGA TAT GGC A	3': Biotin 5': Phosphate
	5'-digoxigenin EcoR1	29 nt	GAA TGT ACG TGA GAA TCG AGA CCC AGG CC	5':Digoxigenin
	5'-digoxigenin EcoR1 linker	33 nt	AAT TGG CCT GGG TCT CGA TTC TCA CGT ACA TTC	-
	Mismatch linker 1	47 nt	Same with above	Same with above
	Mismatch linker 2	47 nt	Same with above	Same with above

Supplementary Table 2. G/T mismatch binding and ATP dissociation activity of HsMSH2-HsMSH6.

Protein	k_{on} ($10^5 \times M^{-1} \times sec^{-1}$)	k_{off} ($10^{-4} \times sec^{-1}$)	K_D (nM)	$k_{off \cdot ATP}$ (sec^{-1})
HsMSH2-HsMSH6 (Wild Type)	9.22 ± 1.39	13.04 ± 3.74	1.43 ± 0.37	0.20 ± 0.07
HsMSH2-HsMSH6 (mEos3.2)	10.99 ± 2.50	11.21 ± 3.74	1.09 ± 0.48	0.68 ± 0.12

Supplementary Table 3. Oligonucleotides used for PIFE.

	Name	Length	Strand Sequence (5' to 3')	Modification
40 bp Duplex Cy3	5'bio_Cy3_oligo	40 nt	CCT GTG TTA GCT CGA GGC TAT GCA TGA C**T**G CTC TTT GAA C	5': Biotin **T**: Amino-dT + Cy3
	5'dig_match	40 nt	GTT CAA AGA GCA GTC ATG CAT AGC CTC GAG CTA ACA CAG	5': Digoxigenin
40bp(+0T) G/T Cy3	5'bio_Cy3	40 nt	Same with above	Same with above
	5'dig_+0T	40 nt	GTT CAA AGA GCA GTC ATG CGT AGC CTC GAG CTA ACA CAG G	5': Digoxigenin
40bp(+10T) G/T Cy3	5'bio-Cy3	40 nt	Same with above	Same with above
	5'dig_+10T	50 nt	T TTT TTT TTT GTT CAA AGA GCA GTC ATG CGT AGC CTC GAG CTA ACA CAG G	5': Digoxigenin
40bp(+30T) G/T Cy3	5'bio-Cy3	40 nt	Same with above	Same with above
	+30T	70 nt	TTT TTT TTT TTT TTT TTT TTT TTT TTT TTT GTT CAA AGA GCA GTC ATG CGT AGC CTC GAG CTA ACA CAG G	-
40bp(+40T) G/T Cy3	5'bio-Cy3	40 nt	Same with above	Same with above
	+40T	80 nt	T TTT TTT TTT TTT TTT TTT TTT TTT TTT TTT TTT TTT TTT GTT CAA AGA GCA GTC ATG CGT AGC CTC GAG CTA ACA CAG G	-

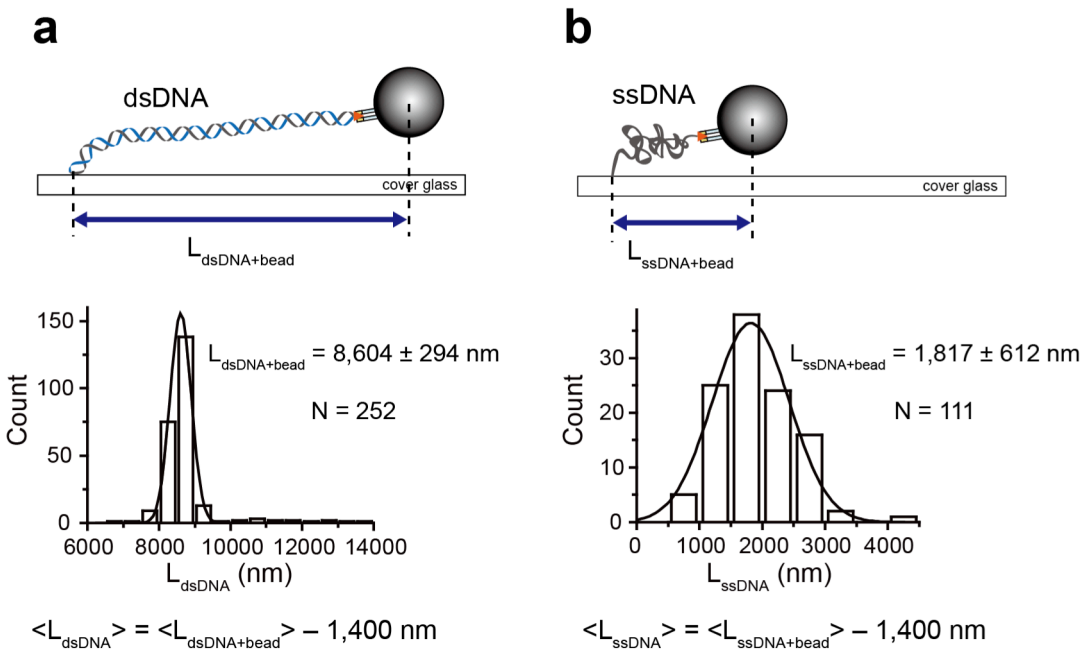

Supplementary Figure 1. Force Extension Difference Between dsDNA and ssDNA. We determined the distance ($L_{dsDNA/ssDNA+bead}$) between one end of DNA (the anchor point on the surface) and the center of the bead by measuring half of the distance between the centers of bead at opposite directions of a buffer flow. **a)** $L_{dsDNA/ssDNA+bead}$ of a 21,845 bp long dsDNA was 8,604 ± 294 nm (mean ± s.d.) at 2.5 pN, obtained from 252 molecules. The end-to-end distance projected on the surface on average ($<L_{dsDNA}>$) was 7,204 nm, which was obtained from the formula of $<L_{dsDNA+bead}>$ (8,604 nm) – bead radius (1,400 nm). **b)** To convert a bead position at the nanometer scale into the number of nucleotides excised by HsEXO1, ssDNA was prepared by denaturing the DNA substrate in a 2 mM NaOH solution at 99°C for 5 min and then immediately quenching it in a cold blocking buffer (~ 4°C) to prevent re-annealing. The end-to-end distance projected onto the surface of 21,845 nt long ssDNA was 417 nm at 2.5 pN, on average (111 molecules), which was obtained with the same method for dsDNA. The error bar indicates s.d. This observation suggests a 6,787 nm difference between the lengths of ssDNA (417 nm) and dsDNA (7,204 nm) under a constant extension force (2.5 pN). The resulting dsDNA → ssDNA conversion factor is then 3.2 nt/nm.

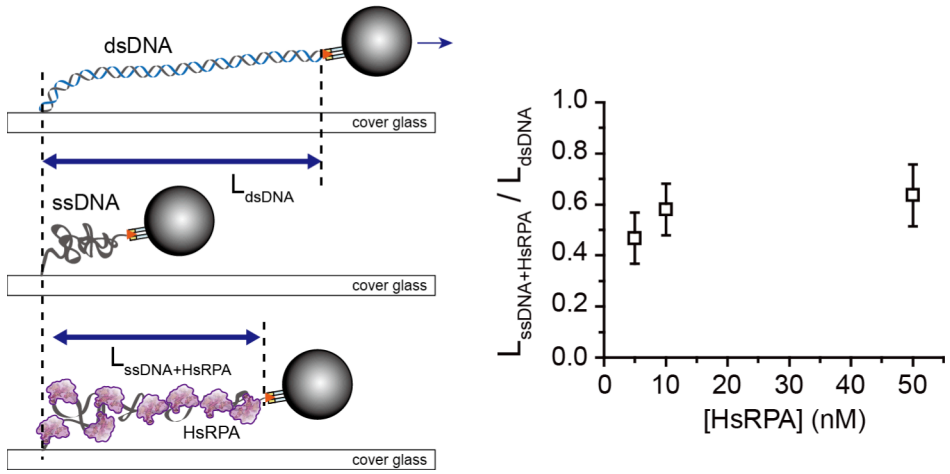

Supplementary Figure 2. Extension of ssDNA Bound by HsRPA. The extension of 21,845 nt ssDNA in the presence of 5, 10 or 50 nM HsRPA at 2.5 pN. N = 17, 19, 15 for 5 nM, 10 nM, 50 nM HsRPA, respectively. The error bars indicate s.d.

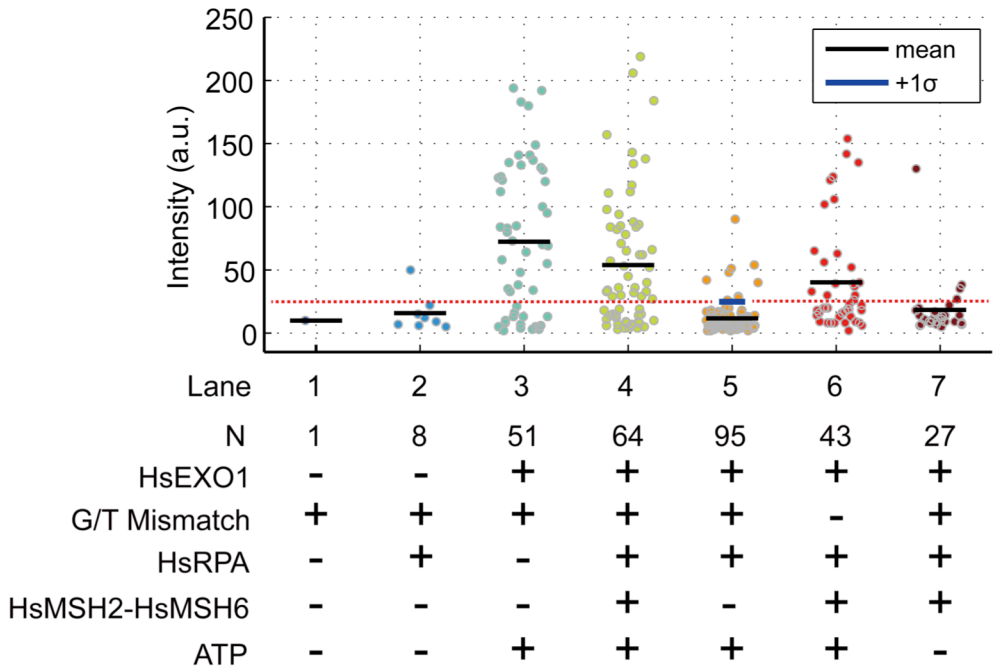

Supplementary Figure 3. Alexa647-HsRPA Emission Intensity with MMR Components. The distribution of the emission intensity of HsRPA detected by Alexa647 labeled anti-HsRPA70 antibody. Protein components (+) were incubated in Buffer A for 60 min followed by single molecule imaging. Red dotted line (blue in Lane 5) indicates average intensity plus one standard deviation (+1σ) of the HsEXOI + HsRPA reaction. Black lines indicate average intensity under described protein conditions. N indicates the total number of DNA molecules containing an Alexa647 focus.

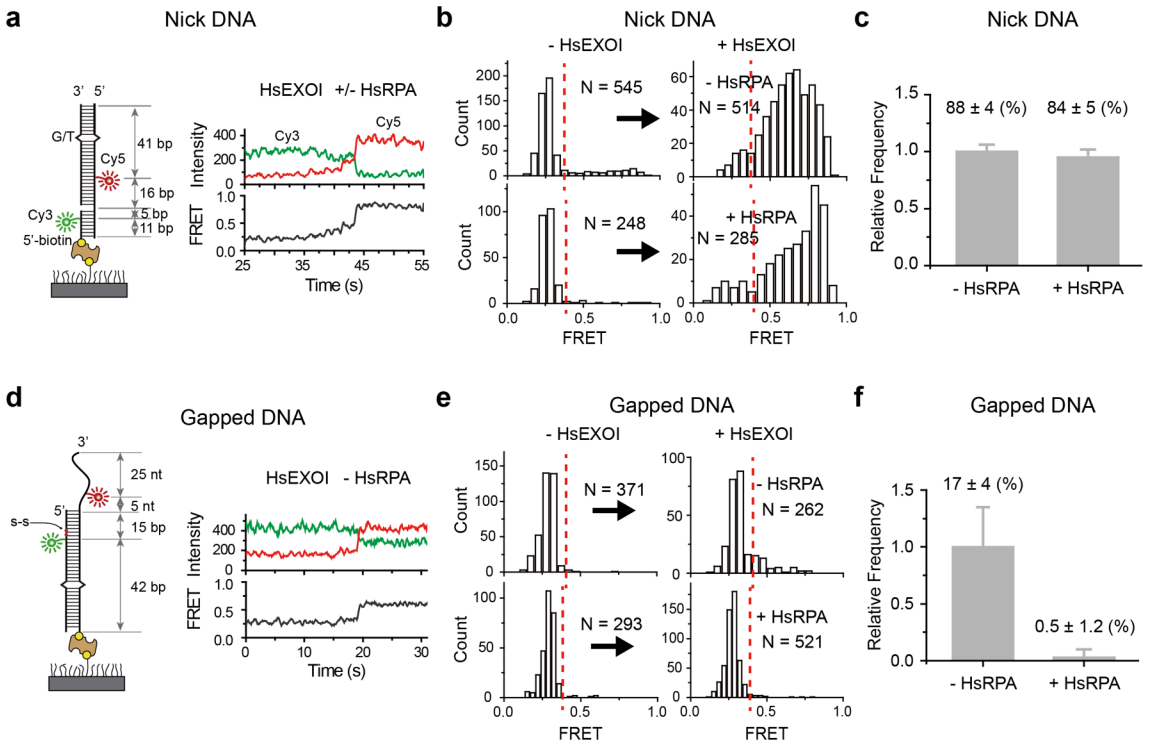

Supplementary Figure 4. Interrogating the Mechanism of HsEXOI inhibition by HsRPA. **a)** Illustration of the model 73 bp DNA containing a strand break (Nick) 5' of the mismatch between a Cy3 donor and Cy5 acceptor pair (left); a representative time trajectory showing the change in Cy3-Cy5 proximity and the resulting increased FRET efficiency during an HsEXOI catalyzed excision reaction that created an ssDNA gap (right). **b)** Histogram analysis of the FRET distribution ± HsEXOI (15 nM) in the presence or absence of HsRPA (10 nM). The number of events analyzed (N) is shown. **c)** The Relative Frequency of excision in the absence (left; Frequency = 462/514) or presence (right; Frequency = 248/285) of HsRPA (before background correction and normalization; see Data Analysis of Relative Frequency). The percentage Frequencies were obtained after the background correction. **d)** Illustration of the model gapped DNA substrate containing a 30 nt 3' ssDNA oligo-dT tail with a Cy5-donor 5 nt from the ssDNA/dsDNA junction, then 14 bp of duplex DNA from the recessed 5'-end terminating in phosphorothioate (S-S) linkages before a Cy3-donor (left); and a representative trajectory resulting in increased FRET efficiency during an HsEXOI catalyzed excision reaction that extended ssDNA gap (right). **e)** Histogram analysis of the FRET distribution ± HsEXOI (15 nM) in the presence or absence of HsRPA (10 nM). **f)** The Relative Frequency of gap extension in the absence (left; Frequency = 46/262) or presence (right; Frequency = 12/521) of HsRPA (before background correction and normalization; see Data Analysis of Relative Frequency). The percentage Frequencies were obtained after the background correction. The error bars indicate the standard error that was determined from at least two independent experiments.

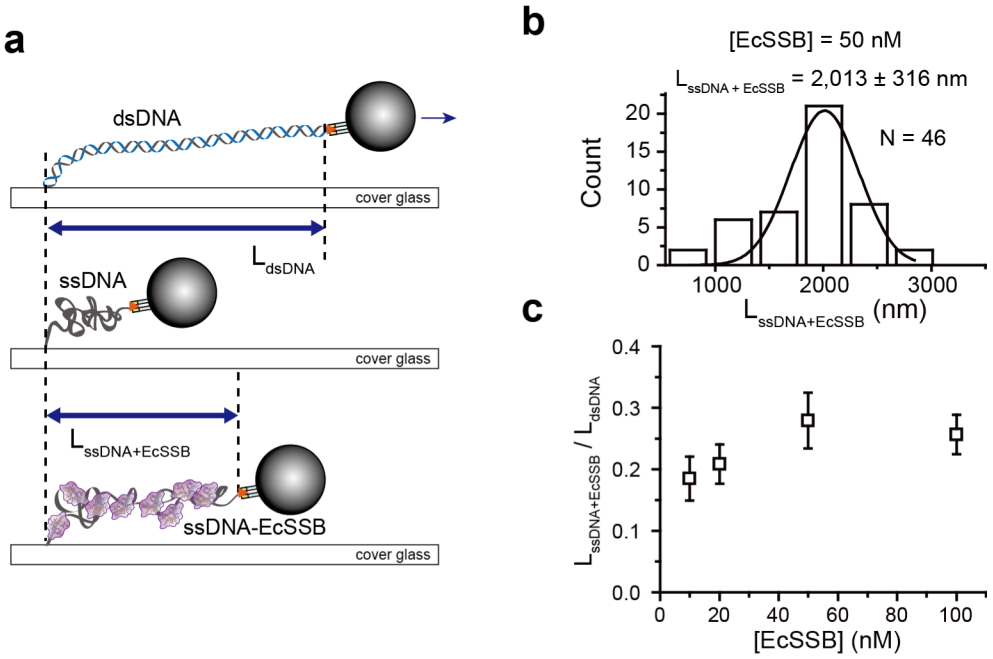

Supplementary Figure 5. Extension of ssDNA Bound by EcSSB. **a)** Schematic illustration of ssDNA extension in the presence of EcSSB. **b)** Binned histogram of ssDNA extension in the presence of EcSSB (50 nM). The average end-to-end distance (<L>) of the EcSSB-ssDNA complex was 2,013 nm. The resulting dsDNA→ssDNA bound by EcSSB (ssDNA-EcSSB) conversion factor is 4.2 nt/nm. **c)** The length ratio of dsDNA to ssDNA at various concentrations of EcSSB (10 nM, N = 21; 20 nM, N = 20; 50 nM, N = 46; 100 nM, N = 31). The error bars indicate s.d.

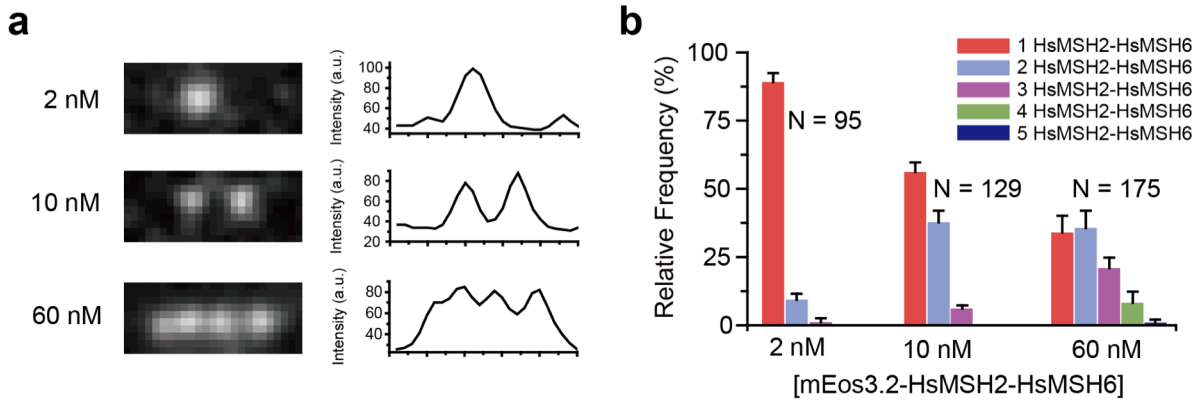

Supplementary Figure 6. The Frequency of HsMSH2-HsMSH6 Sliding Clamps on Mismatched DNA. mEos3.2 photoswitchable fluorescent protein was fused in-frame to the C-terminus of HsMSH2, coexpressed with His_6-HsMSH6 and purified as previously described (1) (see Supplementary Methods). The number of mEos3.2-HsMSH2-HsMSH6 sliding clamps was determined over a 10 min imaging time in Buffer A plus 1 mM ATP and 0.1 mM ADP as previously described (3), on the15.3 kb mismatched DNA tethered on the flow-chamber surface at both ends by 5' biotin. Individual mEos3.2-HsMSH2-HsMSH6 sliding clamps were visualized in the absence of any hydrodynamic force. Before the imaging free proteins were washed out. The mEos3.2 fluorescent protein was photoactivated with a 405 nm laser (Cobolt, 75 mW), its emission signals excited with a laser with 561 nm (Cobolt, 100 mW) and imaged by the identical method used for PIFE (Supplementary Methods). **a)** Images and the intensity profiles of mEos3.2-HsMSH2-HsMSH6 on the mismatched DNA after incubation of 2 nM, 10 nM or 60 nM mEos3.2-HsMSH2-HsMSH6. The signal-to- noise ratio [= (S-BG)/BG_s.d.] is 5.0 on average, for which S = average intensity of 5 X 5 pixels including a center of the peak, BG = average intensity of 5 X 5 pixels far from the signal and BG_s.d. = standard deviation of BG. **b)** For 2 nM and 10 nM mEos3.2-HsMSH2-HsMSH6 analysis, the activation and excitation lasers were continuous. We used a continuous excitation while the activation was on for 50 ms and off for 450 ms for 60 nM mEos3.2-HsMSH2-HsMSH6 analysis. Standard error was determined from at least four independent experiments.

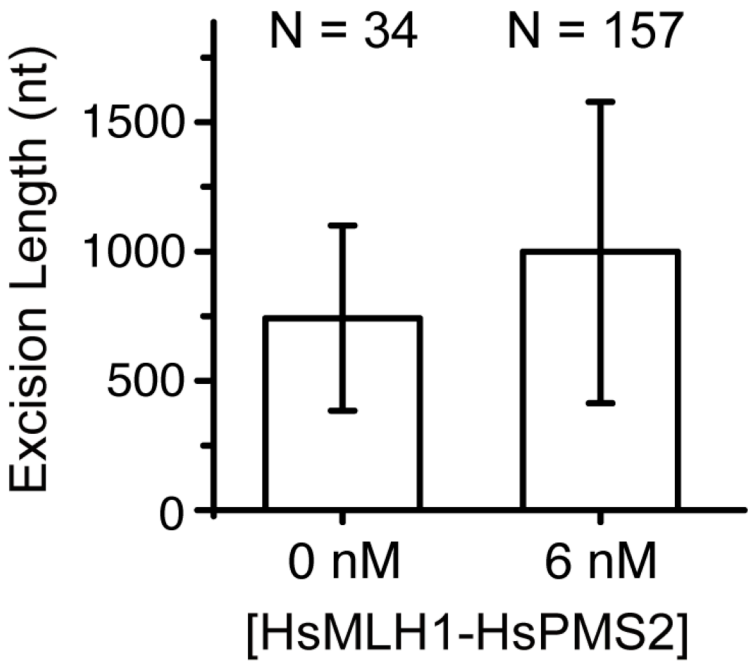

Supplementary Figure S7. HsMLH1-HsPMS2 Does Not Decrease the Excision Length of HsEXOI with Preassembled HsMSH2-HsMSH6. HsMSH2-HsMSH6 (2 nM) was introduced into a flow chamber containing immobilized 15.3 kb G/T mismatched DNA molecules for 10 min, as shown in Fig. 1. This preassembly will result in a single HsMSH2-HsMSH6 sliding clamp on 90% DNA molecules (see Fig. S6). The infusion of HsEXOI (3 nM), HsMLH1-HsPMS2 (0 nM or 6 nM) and 50 nM EcSSB initiates excision reaction, which was followed for 30 min. The distribution of excision lengths at was fitted to a Gamma distribution. The error bars indicate s.d.

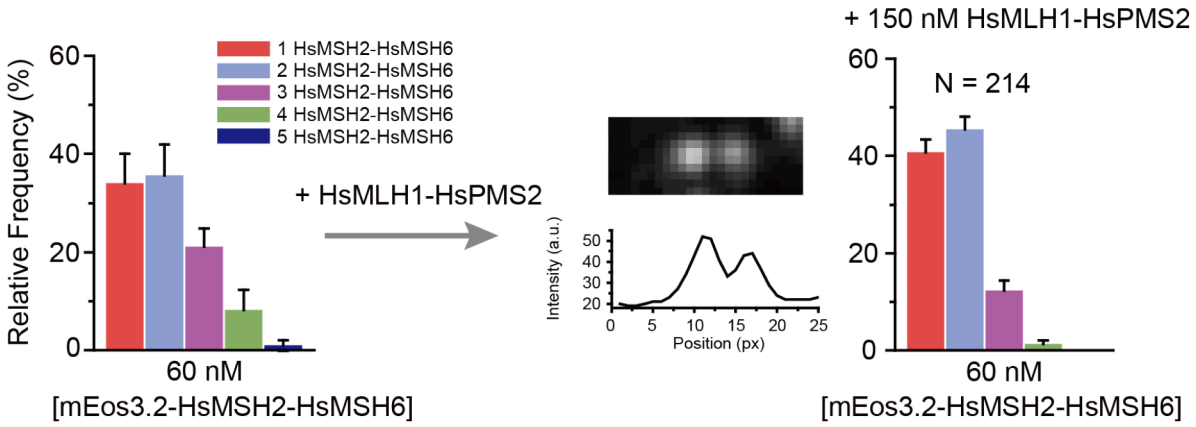

Supplementary Figure 8. The Number of mEOS3.2-HsMSH2-HsMSH6 Sliding Clamps on a Mismatch DNA is Regulated by HsMLH1-HsPMS2. Left) The number of HsMSH2-HsMSH6 (60 nM) sliding clamps on a single 15.3 kb mismatched DNA molecule. **Middle)** Image and its intensity profile in the presence of 60 nM mEos3.2-HsMSH2-HsMSH6 and 150 nM HsMLH1-HsPMS2. The signal to noise ratio is 3.6 (see Suppl. Fig. S6). **Right)** The number of HsMSH2-HsMSH6 (60 nM) sliding clamps on a single 15.3 kb mismatched DNA molecule in the presence of HsMLH1-HsPMS2 (150 nM). Standard error was determined from at least five independent experiments performed in Buffer A.

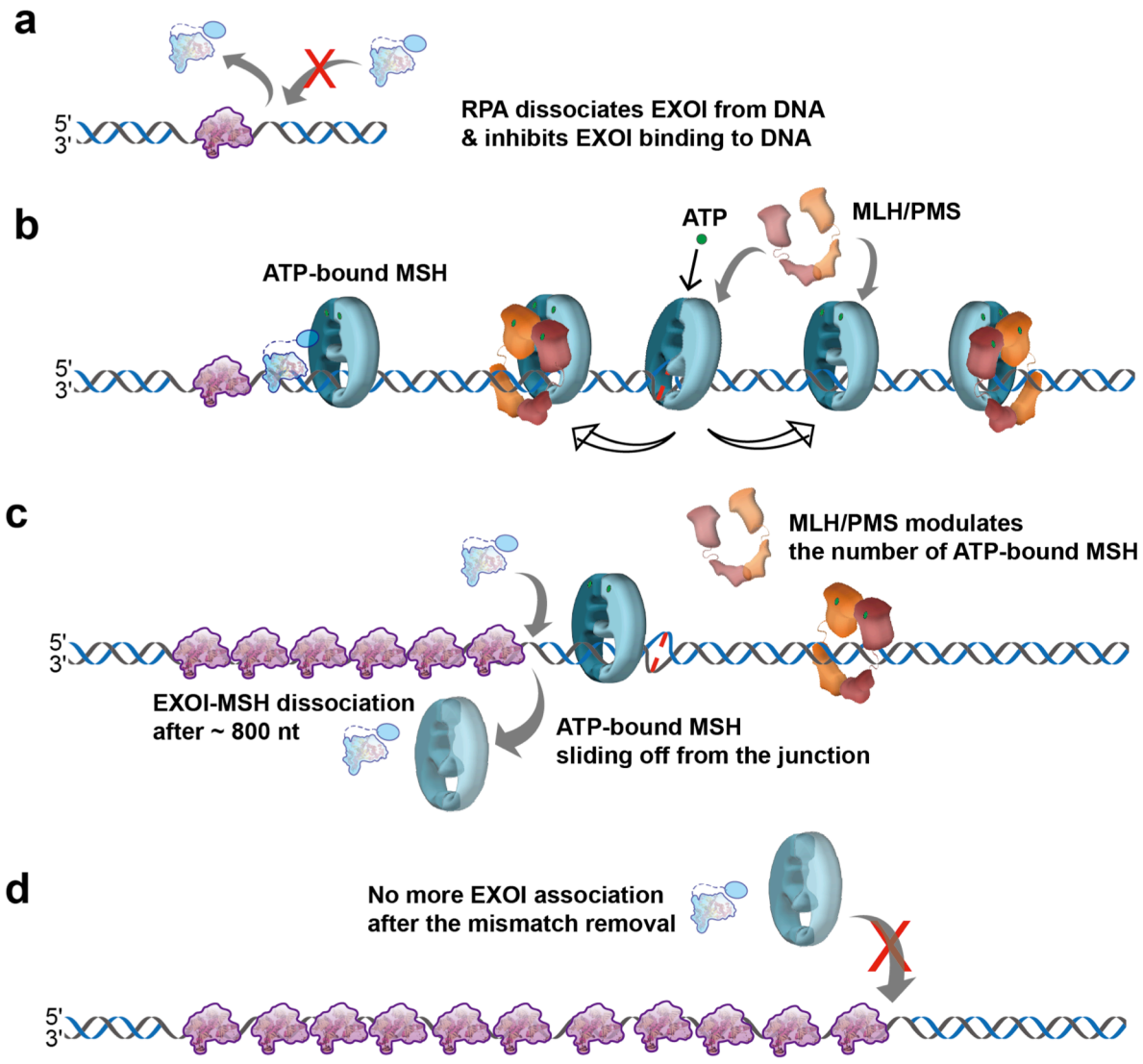

Supplementary Figure 9. A Model for 5'-Mismatch Repair. a) HsRPA binding to an ssDNA gap either produced by RNA-primer removal or HsEXOI excision for a single strand scission, inhibits further excision by HsEXOI. **b)** The presence of a mismatch provokes the loading of multiple ATP-bound HsMSH2-HsMSH6 sliding clamps that may become associated with HsMLH1-HsPMS2. Diffusion of HsMSH2-HsMSH6 to the site of the 5' strand scission bound by HsRPA activates HsEXOI. **c)** HsMSH2-HsMSH6/HsEXOI excision continues for an average of 830 nt before the complex dissociates. A second then third HsMSH2-HsMSH6 initiates excision by complexing with HsEXOI. In the absence of MMR excision activity and/or other downstream components HsMLH1-HsPMS2 stochastically modulates HsMSH2-HsMSH6 sliding clamps reducing run-away excision. **d)** Once the mismatch is removed, additional HsMSH2-HsMSH6 sliding clamps are unable to load, while HsRPA binds the ssDNA excision tract inhibiting further HsEXOI exonuclease activity.

REFERENCES

1. Gradia S, Acharya S, & Fishel R (1997) The human mismatch recognition complex hMSH2-hMSH6 functions as a novel molecular switch. *Cell* 91(7):995-1005.

2. Heinen CD*, et al.* (2011) Human MSH2 (hMSH2) protein controls ATP processing by hMSH2-hMSH6. *J Biol Chem* 286(46):40287-40295.

3. Jeong C*, et al.* (2011) MutS switches between two fundamentally distinct clamps during mismatch repair. *Nat Struct Mol Biol* 18(3):379-385.

4. Henricksen LA, Umbricht CB, & Wold MS (1994) Recombinant replication protein A: expression, complex formation, and functional characterization. *J Biol Chem* 269:11121-11132.

5. Amunugama R*, et al.* (2012) RAD51 Protein ATP Cap Regulates Nucleoprotein Filament Stability. *J Biol Chem* 287(12):8724-8736.

6. Cho WK*, et al.* (2012) ATP alters the diffusion mechanics of MutS on mismatched DNA. *Structure* 20(7):1264-1274.

7. Park J*, et al.* (2010) Single-molecule analysis reveals the kinetics and physiological relevance of MutL-ssDNA binding. *PLoS One* 5(11):e15496.

8. Vallotton P & Olivier S (2013) Tri-track: free software for large-scale particle tracking. *Microsc Microanal* 19(2):451-460.